AIAA JOURNAL
Vol. 41, No. 5, May 2003

Application of Vorticity Confinement to Prediction of the Flow over Complex Bodies

Y. Wenren*
Flow Analysis, Inc., Tullahoma, Tennessee 37388
and
M. Fan,† L. Wang,‡ M. Xiao,‡ and J. Steinhoff§
University of Tennessee Space Institute, Tullahoma, Tennessee 37388

The vorticity confinement technique, which represents a very effective, unified way of treating complex, high-Reynolds-number separated flows with thin convecting vortices, as well as thin attached boundary layers, over complex solid bodies. Conventional Eulerian computational methods are discussed and then contrasted with vorticity confinement, which is also Eulerian. The basic assumptions in vorticity confinement, are reviewed, and then the method itself is briefly outlined. Following the description, representative results are presented: First, two-dimensional results for convecting vortices and Cauchy–Riemann flow over a cylinder are presented. These describe, respectively, the salient features of the method for convecting vortices and for flow over solid surfaces, embedded in a uniform Cartesian grid. Then, three-dimensional results for flow over complex configurations, including a complete rotorcraft, are presented.

I. Introduction

MOST high-Reynolds-number incompressible flows are characterized by vortical structures that are either fixed, such as attached body-conforming boundary layers, or separate and convect, such as wakes. These structures can often be turbulent and are typically approximately modeled by partial differential equations (PDEs), as in eddy viscosity approaches. In this context, we can also consider inviscid discretized Euler PDEs to be crude models. These structures are often very thin, and conventional methods using model PDEs are then very difficult to solve due to resolution problems. These difficulties result in costly solution strategies involving body-fitted grids, often with extensive refinement near the body surface, and adaptive grids with extensive refinement within shed vortex sheets and filaments, if any pretense is to be made of accurately resolving the model PDEs within these regions.[1]

In this paper, we describe a much more efficient way of computing many of these features, including attached boundary layers and separating vortex sheets and filaments. Once we realize that these PDEs are only approximate models for these vortical regions, we are led to the idea of modeling them directly on the grid using (nonlinear) difference equations, rather than using finite difference equations that attempt to resolve the model PDEs approximately. This approach allows us to treat these structures as near-singular objects spread over only a few grid cells on an essentially uniform Cartesian computational grid.

In these computations, the main goal is often not to compute the internal details of these structures, but their effect on the outer main flowfield. This idea is, of course, what is commonly used in shock-capturing algorithms as an alternative to computing a detailed Navier–Stokes solution for the internal shock structure. However, shocks involve characteristics that point inward, unlike vortical structures, making them easy to capture.

Received 28 November 2000; revision received 13 September 2002; accepted for publication 13 December 2002.

*Senior Research Scientist. Member AIAA.
†Research Scientist, Mechanical and Aerospace Engineering and Engineering Science Department. Member AIAA.
‡Research Assistant, Mechanical and Aerospace Engineering and Engineering Science Department.
§Professor, Mechanical and Aerospace Engineering and Engineering Science Department. Member AIAA.

The vorticity confinement method, which implements this approach for vortical structures, as opposed to shocks,[2,3] has proven to be a particularly effective technique to treat both body-conforming boundary layers and shed vortex sheets and filaments. At the current stage of development, very simple structures are modeled for these vortical regions. These are adequate for the problems treated to date, which involve only thin attached boundary layers and separation from sharp corners and thin convecting vortex sheets and filaments. More sophisticated models are currently being developed to treat turbulent boundary layers separating from smooth surfaces.

With the method, solutions are computed on a relatively coarse (typically uniform Cartesian) grid. Even though the method is completely Eulerian, with no Lagrangian marker arrays, shed vortex filaments can be convected indefinitely with no numerical spreading, even though they are only a few grid cells in diameter. As such, vorticity confinement has the control over vortical structures that Lagrangian "vortex tracking" schemes have. On the other hand, as in conventional Eulerian techniques, the method allows vortex sheets to automatically be shed or reattach and vortex filaments to merge or reconnect with no logical operations or redistribution of marker arrays, which are typically required in Lagrangian schemes. Furthermore, the method allows the embedding of complex solid surfaces in these grids with no requirement for complicated grid refinement, complicated logic, or multiple body-fitted grids.

In this paper, some comments concerning conventional methods are first made, and the vorticity confinement method is outlined. Representative results are then presented for flows with the preceding features involving bound and convecting vorticity. These demonstrate the basic capabilities of the method, as described earlier. Finally, computations for complex three-dimensional configurations are presented.

II. Conventional Eulerian Method

We only consider high-Reynolds-number flows where turbulent regions must be modeled. The goal is to suggest a new approach for these flows that may prove to be much more efficient than current ones.

A large amount of work has been done by many people over decades in developing computational fluid dynamics (CFD) methods. For low-speed flows, highly accurate higher-order methods have been developed for low-Reynolds-number, viscous flows, where all of the relevant scales can be treated by resolving the physical Navier–Stokes equation. Our method is not meant to be used in these cases.

Also, a large amount of work has been done on developing PDE-based turbulence models (typically involving a modeled eddy viscosity coefficient multiplying second derivative terms). These models can contain a number of separate PDEs and constants that have been tuned to match a number of flows. At present, these obviously represent the only approach for getting engineering accuracy for many flows. We emphasize that our purpose is not to propose an immediate replacement for these models. Instead, we hope to demonstrate a new approach that, given sufficient additional modeling efforts, can lead to a far more efficient method with far less grid generation and computation. The results presented are meant to demonstrate that even our very simple, initial formulation gives very good results, so that we should expect success from such a program.

Typically, in conventional computations, PDEs are first formulated that express the equations of motion of the fluid. These equations can include explicit models for the turbulent regions. Although the following point may seem trivial, it is important to emphasize it: If we consider thin vortical regions at high Reynolds number, either attached (boundary layers) or separated (convecting vortices), for realistic configurations, the goal is always to model these regions (or even ignore them as in inviscid treatments of solid boundaries). This is, of course, because they can be mostly turbulent and a direct Navier–Stokes computation, including the small turbulent scales, is out of the question. This modeling can be explicit, such as, for example, Navier–Stokes-like PDEs with an eddy viscosity model and possibly other related transport PDEs. Alternatively, if the vortical regions are regarded as so thin that the details of the internal structure are not important for determining the overall, outer irrotational flows, discretized inviscid Euler equations can be used and the computed results only taken to be a crude model of the vortical regions. Our main point is that, whether the discretized Euler equations or Navier–Stokes-like equations with a model viscosity are used, the result is still a model for the vortical regions at high Reynolds number.

Of course, Lagrangian vortex lattice methods[4–6] also constitute a model of, for example, the internal structure of a rolling up vortex sheet or a solid surface. Also, the Lagrangian "vortex blob" approach models the internal structure.[7] Furthermore, early approaches using analytic methods,[8,9] involved treating a vortex sheet as an exact contact discontinuity. These methods can also be thought of as models for the actual internal vortical structure.

The main feature that we want to bring out about conventional methods is that, although they involve an efficient discretization and solution of the irrotational or outer part of the flowfield, they also involve an inefficient model for thin vortical regions: When a PDE (or set of PDEs) is first formulated as an approximate model and then must be discretized and accurately solved in thin regions, great computational difficulties can arise. Manifestations include having to use very dense grids for convecting vortices, or fine adaptive grids that require large computational time to "grow" and follow the vortical region so that the discretized PDEs can be resolved.[10] Even after this effort, the result is still a model approximation. Furthermore, the conventional treatment of solid boundaries even in the inviscid approximation requires high accuracy at the surface. Otherwise, numerical errors, usually in the form of numerically generated vorticity, can be created and diffuse or convect away from the surface, contaminating the solution. The impact on computational requirements is great: Either surface-conforming grids must be used, which are difficult to generate for complex geometries, or nonconforming Cartesian grids can be used with extensive (nonuniform) refinement at the boundary.

Another problem is that it is difficult to see how these models can be discretized and accurately solved (that is, in a grid independent limit) for separating flow from smooth surfaces. Even the simplest case, laminar two-dimensional Navier–Stokes equations in the thin boundary-layer approximation for a circular cylinder, have proven to be very difficult to solve.[11] Furthermore, because vortical structures with size comparable to the total thickness are important in the boundary layer, it is difficult to see how an eddy viscosity approach, which is the basis of PDE-based models, is appropriate. Thus, current PDE models for approximating Reynolds-averaged turbulent flow may not be a good approach, for both computational and physical reasons, and perhaps a different type of modeling should be considered.

A final point concerns consistency in accuracy for flows involving nearby separating vorticity, where the flow near the surface is a function of the separated, convecting vorticity as well as the bound, attached vorticity. In many conventional methods, the bound and separating vorticity are treated differently (the bound with conforming or locally refined grids, and the separating without, because the problem of locally refining the grid near a thin convecting vortex is much greater than for a fixed surface[1,10]). This disparity could negate any benefit of using highly accurate conforming grids near a surface because the final accuracy of the solution cannot be better than that for the nearby convecting vorticity, which may not involve a conforming grid or local refinement.

III. Vorticity Confinement

A. Requirements

The main goal of vorticity confinement is to model thin vortical regions using only a few grid points in the cross section, without requiring them to be aligned with the grid. The method must allow vortices to be convected over long distances with no numerical spreading and must allow merging of convecting vortices and other changes in topology. It must have the ability to convect vorticies over objects and reconnect or, for vortex sheets, to separate and reattach. In addition, it must also allow complex solid surfaces, such as thin, fixed vortex sheets, to be easily embedded in a uniform Cartesian grid.

B. Basic Concept

The basic idea behind vorticity confinement is to develop a set of difference equations on a fixed grid (typically uniform Cartesian) that fulfill the preceding requirements. This implies that the equations must be an accurate discretization of the Euler PDEs in the outer, irrotational regions but reduce to a set of difference equations (as opposed to finite difference approximations of PDEs) in the vortical regions where flow quantities vary by $\mathcal{O}(1)$ over a few grid cells. Furthermore, to allow separation, reattachment, merging, etc., the vortical structure can not be specified. Instead, the structure must relax to the desired profile.

The preceding requirements mean that there should be two basic parameters in the method, a length scale and a timescale. These are directly related to the grid cell size and time step of the computation, that is, the resulting vortical profile should be a few grid cells wide, and the relaxation should take place over a small number of time steps. Of course, if relevant, more complex models (including, for example, boundary-layer dynamics or long-term viscous spreading) must be implemented that would involve more parameters. These are currently being formulated for cases with separation from smooth surfaces.

Some of the basic ideas are demonstrated for the advection of thin pulses in one dimension in Ref. 12, where the pulses are essentially treated as discrete solitary waves that propagate indefinitely without changing shape.

C. Formulation

The simplest formulation of vorticity confinement involves, for general, unsteady incompressible flow, adding two terms to the discretized momentum conservation equations in a primitive variable formulation, which are similar to the diffusion and nonlinear antidiffusion term for the advecting short pulse discussed in Ref. 12. These terms are inherently multidimensional and Galilean invariant, depend only on local variables, and vanish outside the vortical regions.

The governing equations with the vorticity confinement terms are then a discretization of the following equations:

$$\nabla \cdot \boldsymbol{q} = 0$$

$$\partial_t \boldsymbol{q} = -(\boldsymbol{q} \cdot \nabla)\boldsymbol{q} - \nabla(p/\rho) + [\mu \nabla^2 \boldsymbol{q} - \varepsilon \boldsymbol{s}]$$

where $\boldsymbol{q}$ is the velocity vector, p pressure, and ρ density. The two terms in brackets are the confinement terms. The two numerical coefficients, ε and μ, control the size of the convecting vortical

regions or vortical boundary layers and their relaxation rate to a quasi-steady shape.

There are many possible forms for the second confinement term. The simplest one seems to be

$$\boldsymbol{s} = \hat{n} \times \boldsymbol{\omega}$$

where

$$\hat{n} = \nabla\eta/|\nabla\eta|$$

The vorticity vector is given by

$$\boldsymbol{\omega} = \nabla \times \boldsymbol{q}$$

The scalar field η is defined in two ways:

$$\eta = \begin{cases} |\omega| : \text{field confinement} \\ |F| : \text{surface confinement} \end{cases}$$

The simplest implementation of vorticity confinement, for convecting vortices, is called field confinement. A simple modification, surface confinement, for boundary layers will be described in the next section.

For field confinement, the unit vector $\hat{\eta}$ points toward the local centroid of the vortical region, and the confinement term serves to convect vorticity back toward the centroid as it diffuses away. This convection increases the diffusion term, and a steady-state distribution automatically results when the two terms become balanced (for any reasonable values of μ and ε). Additional discussions of the formulation can be found in Refs. 3, 13, and 14.

An important feature of the vorticity confinement method is that the extra terms are limited to the vortical regions: Both the diffusion term and the confinement term vanish outside those regions (in the continuum limit, which should be accurate there). Another important feature concerns the total change induced by the correction in mass, vorticity, and momentum, integrated over a cross section of a convecting vortex sheet or filament. It is shown in Refs. 3, 13, and 14 that mass and vorticity are explicitly conserved and momentum is almost exactly conserved. A small extension of the method, described in Sec. III.E.4 and in Ref. 15, allows it to also conserve momentum explicitly. This has no observable effect on most results, except for cases involving long-term convection of vortices in a low velocity field. Then, the momentum conserving extension is easily implemented to ensure accurate trajectories.

In general, computed flows do not depend sensitively on the parameters ε and μ for a range of values. Hence, the issues involved in setting them are similar to those involved in setting numerical parameters in other standard CFD schemes, such as artificial dissipation in many conventional compressible solvers that capture shocks. The main effect of varying ε and μ, within a range, is to vary the vortex core radius, which is approximately equal to μ/ε (Ref. 16).

The reason for this lack of sensitivity is that, for example, if a vortex core is close to axisymmetric, the velocity outside the core is not sensitive to the vorticity distribution or core size, as long as the radius is kept small and prevented from becoming large due to numerical effects. This is a well-known property of axisymmetric, parallel vortices. It means that their mutual interaction will also be independent of the structure, as long as they are separated. Because merging, etc., takes place on convective timescales, this is also not sensitive in Ref. 3. This lack of sensitivity to ε was demonstrated for a rolling-up vortex sheet computation[13] where ε was varied by a factor of four and the result remained close to experiment, whereas for $\varepsilon = 0$, the result was much too diffusive.[17] This was also shown in Ref. 18 for dynamic stall. Similar considerations apply to thin boundary layers. (This is analogous to the artificial shock thickness effects that depend on the dissipation parameter.) This is explained in Sec. III.F.

In addition to the solitary wavelike features of the vorticity distribution for free convecting vortices in two and three dimensions, (convection with fixed shape), two studies, Refs. 3 and 14, demonstrated the ability of convecting three-dimensional vortex filaments, initially in the form of rings, to merge and reform. A comparison of these results[3] with measurements from an experiment[14] showed a very close agreement. This demonstrated that the basic computational concept of relaxing to a quasi-steady vortical state through the action of the diffusion and nonlinear terms automatically allows realistic vortex filament reconnection, while at the same time preventing spreading due to numerical effects. This is true even though a coarse grid was used where the vortex cores were only ~3 grid cells in diameter.

It has been shown numerically that vortical solutions to the discretized equations are qualitatively close to those predicted for the continuum ones, even though the vortical regions are only a few cells thick. Roughly speaking, the confinement terms seem to be convecting discretization errors into the vortex center. This point should be addressed by an analysis of the discrete equations themselves, which we are currently carrying out.

Finally, note that these solutions should be considered as zeroth-order solutions, which are very economical but do not take into account dynamics in the vortical cores, such as turbulence effects. The idea is to include such effects, if they are significant, in a perturbative way using extensions of the confinement method. In this way, vorticity confinement can be regarded as a new type of framework for fluid dynamic computations.

D. Solid Surface Modeling with Uniform Cartesian Grids

The application of vorticity confinement to fixed vortex sheets representing solid surfaces in a nonconforming regular Cartesian grid with no-slip boundary conditions has recently been presented in Refs. 12 and 19–22. This represents a very simple, economical way to treat complex bodies because it does not require body-conforming or adaptive grid generation and can use a fast Cartesian grid setup and flow solver. The steps for this method are delineated here:

1) The geometry of the body or free surface is specified in a conventional way, such as by the coordinates of a set of points on the surface.

2) From this set of points, a smooth function is computed on each point of a regular Cartesian computational grid. The value of this function, $F(\boldsymbol{x})$, is the (signed) distance of the grid point to the defined surface. Thus, the "level set" of values of $\boldsymbol{x}$ such that $F(\boldsymbol{x}) = 0$ implicitly defines the surface over which the flow is to be solved. This $F = 0$ surface (defined implicitly) can be complicated and even move according to dynamic equations.

3) The flow over the $F = 0$ surface is computed time accurately in a sequence of time steps. This involves confining vorticity to the (fixed) $F = 0$ surface, as well as the convecting vortical regions.

E. Computational Details

For each time step n, the following computations are executed:

1. *Step a: Velocity Damping in Body*

The velocity, $\boldsymbol{q}^n$ is multiplied by a function of F; $\lambda(F)$, such that it is reduced for $F < 0$. This factor increases to one near the surface, and no reduction is made in the new velocity at further distances:

$$\boldsymbol{q}' = \lambda(F)\boldsymbol{q}^n$$

2. *Step b: Convection*

A convectionlike computation is made to treat part of the momentum equation, as in conventional incompressible "split velocity" methods.[23] This is a space-discretized version of

$$\boldsymbol{q}'' = \boldsymbol{q}' - \Delta t \boldsymbol{q}' \cdot \boldsymbol{\nabla} \boldsymbol{q}'$$

Both conservative and nonconservative discretizations have been used for this step. Little difference has been seen.

3. *Step c: Confinement*

Vorticity confinement is used to compute a velocity increment such that quasi-steady thin vortical structures are obtained:

$$\boldsymbol{q}''' = \boldsymbol{q}'' + \Delta t\left(\varepsilon_f \hat{n}_f \times \boldsymbol{\omega} - \varepsilon_\omega \hat{n}_\omega \times \boldsymbol{\omega} + \mu \nabla^2 \boldsymbol{q}''\right) \qquad (1)$$

Here $\boldsymbol{\omega}$ is vorticity and

$$\hat{n}_f = \nabla|F|/|\nabla F|, \qquad \hat{n}_\omega = \nabla|\boldsymbol{\omega}|/|\nabla|\boldsymbol{\omega}||$$

This is a crucial step: It advects vorticity back toward the $F=0$ surface and convecting vortical regions. Without it, vorticity would continually diffuse away leading effectively, to, a highly viscous low-Reynolds-numbersolution because only large regular grid cells are used, rather than very thin body-fitted or adaptively refined cells as in conventional computations. In earlier studies, the preceding diffusion was not added explicitly but resulted from discretization of step b.

In this step, $\varepsilon_f(F)=\varepsilon$, a constantnear $F=0$. It becomes small for points more than two cells away from the body. Also, $\varepsilon_\omega=\varepsilon-\varepsilon_f$.

The details of the discretization of this step are important. It is well known that certain types of discretization are important for stable convection (step b), which can involve an upwind differencing in the direction of the velocity vector. Here, we have the same consideration because this step effects the convection of vorticity, although in the direction of $\hat{n}$.

We first use a box scheme to compute vorticity in each cell center. We describe the method in two dimensions for simplicity. The three-dimensional implementation is a straightforward extension:

$$\omega_{ij}=-(1/2h)[u_{i,j+1}+u_{i+1,j+1}-v_{i+1,j+1}-v_{i+1,j}$$
$$-u_{i+1,j}-u_{i,j}+v_{i,j}+v_{i,j+1}]$$

where h is the grid cell size and u_{ij} and v_{ij} are the velocity components at the node (i, j).

The gradient is then computed at the cell node using a box scheme. For these computations, smoothed values of ω are used (ω^s) to ensure a smooth $\hat{n}$ field. Original values are used otherwise:

$$\omega^s_{ij}=\tfrac{1}{8}|(\omega_{i+1,j}+\omega_{i-1,j}+\omega_{i,j+1}+\omega_{i,j-1}+4\omega_{ij})|$$

$$\nabla\omega^s_{i,j}=(1/2h)\begin{pmatrix}\omega^s_{i+1,j}+\omega^s_{i+1,j+1}-\omega^s_{i,j}-\omega^s_{i,j+1}\\ \omega^s_{i,j+1}+\omega^s_{i+1,j+1}-\omega^s_{i,j}-\omega^s_{i+1,j}\end{pmatrix}$$

Then, the unit vector

$$\hat{n}=\nabla\omega^s/|\nabla\omega^s|$$

is computed.

The confinement velocity increment defined in this step [Eq. (1)] is on a cell node rather than a cell center. A "downhill" weighting depending on $\hat{n}$ and surrounding ω values is then used to compute the ω value used in Eq. (1). In two dimensions, this is

$$\bar{\omega}_{i,j}=\sum_{l=1}^{4}\sigma_l\omega_l\Big/\sum_{l=1}^{4}\sigma_l$$

where l labels the cell center points surrounding node i, j. The weighting factors are

$$\sigma_l=\max(0,\hat{n}_{ij}\cdot\hat{d}_l)$$

where

$$\hat{d}_l=(\boldsymbol{x}_l-\boldsymbol{x}_{ij})/|\boldsymbol{x}_l-\boldsymbol{x}_{ij}| \tag{2}$$

and $\boldsymbol{x}_{ij}$ and $\boldsymbol{x}_l$ are the coordinate values of the node i, j and surrounding cell centers, respectively.

4. Step d: Conservative Extension

When it is important, a conservative extension can easily be implemented so that

$$\sum_{i,j}\delta\boldsymbol{q}_{ij}=0 \tag{3}$$

where $\delta\boldsymbol{q}_{ij}$ is the total confinement increment. We start with the nonconservative version as defined in Eq. (1):

$$\delta\boldsymbol{q}^0_{ij}=\varepsilon_\omega\hat{n}_{ij}\omega_{ij}$$

where we use two-dimensional notation for simplicity and just consider field confinement for convecting vortices. The Laplacian part of the confinement term automatically satisfies relation (3) and is not considered.

We then use weighting factors to compute a $\delta\boldsymbol{q}'_{ij}$ such that

$$\sum_{i,j}\delta\boldsymbol{q}'_{ij}=\sum_{i,j}\delta\boldsymbol{q}^0_{ij},\qquad \delta\boldsymbol{q}'_{ij}=\sum_{l=1}^{4}\hat{\sigma}_l\delta\boldsymbol{q}^0_{ij} \tag{4}$$

in which

$$\hat{\sigma}_l=\max\left[\frac{0,(\hat{n}_l\cdot\hat{d}_l)}{S_l}\right],\qquad S_{ij}=\sum_{l=1}^{4}\max[0,(\hat{n}_l\cdot\hat{d}_l)]$$

where l refers to the four grid nodes $i\pm1$ and j and i and $j\pm1$ rather than the four cell centers used for $\bar{\omega}$. The definition of $\hat{d}_l$ [Eq. (2)] is the same with this modification, although different points are used, as described earlier.

The reason that this extension is effective is that the basic values $\delta\boldsymbol{q}^0$ increase as the vortex center is approached (because ω does). Subtracting $\delta\boldsymbol{q}'$ transferred from a point away from the center [using Eq. (4)] results in a total $\delta\boldsymbol{q}=\delta\boldsymbol{q}^0-\delta\boldsymbol{q}'$ that is close to the original $\delta\boldsymbol{q}^0$ because $\delta\boldsymbol{q}'$ is smaller, and the overall effect of convecting ω is still about the same for compact vortical structures.

The resulting confinement term is then a discretized approximation of

$$\mu\nabla^2\boldsymbol{q}+\varepsilon_\omega\boldsymbol{\nabla}\cdot(\hat{n}_\omega\hat{n}_\omega\times\boldsymbol{\omega})$$

Although the effect on confinement of thin vortex filaments is still the same, this modification reduces the effect [by $\mathcal{O}(h)$] on large-scale smooth vortical distributions (if there are any), making this version more suitable for flows where a range of length scales exist. This is not relevant for problems considered in this paper that have only two length scales, vortical scale $\sim\mathcal{O}(h)$ and body or flow scale $\sim\mathcal{O}(1)$.

5. Step e: Pressure Computation

A pressure is computed such that the velocity at time step $n+1$ is divergence free:

$$\nabla\cdot\boldsymbol{q}^{n+1}=0$$

This involves solving a Poisson equation

$$\nabla^2\phi=-\nabla\cdot\boldsymbol{q}'''$$

as in a conventional split velocity procedure.

6. Step f: Velocity Update

The velocity at the next time step is computed:

$$\boldsymbol{q}^{n+1}=\boldsymbol{q}'''+\nabla\phi$$

This agrees with the momentum equation (to first order in Δt) where ϕ is related to pressure by

$$\phi=-\Delta tp/\rho$$

F. Properties of Converged Solution

At convergence, the discrete approximations to $\nabla\cdot\boldsymbol{q}$ and $\nabla\times\boldsymbol{q}$ are driven to zero inside the body. Also, $\boldsymbol{q}$ is forced to zero in a region inside the body. The only solution inside the body is then $\boldsymbol{q}=0$. Because $\nabla\cdot\boldsymbol{q}=0$ everywhere, there is then no flow through the body surface, and vorticity is confined to thin regions on the body surface and thin regions that separate and convect with the flow. These regions are 2–3 grid cells thick, independent of the grid cell size or number of grid points in the overall problem (in the fine-grid limit when $h\ll$ radius of curvature). Furthermore, because the computed velocity has zero divergence, if the separation locations are accurate, the computed velocity field will be at least first-order accurate in the grid cell size both away from convecting vortices and away from the body surface. The first-order error is due to the thickness of the computed vortical regions: Simple perturbative corrections to bring the solution to second-order accuracy can be

formulated within the framework of the method by considering the error as a displacement-thickness effect. This procedure should be simpler for many cases than resorting to the generation of a body-conforming grid or adaptive high-order refinement. However, for blunt body flows with separation, the first-order accuracy should be more consistent with the accuracy of the computation of the separating vorticity.

IV. Current Results

A. Convecting Vortices

As a basic test of the ability of vorticity confinement to convect concentrated vortices accurately and efficiently, we tested the method for two cases in two dimensions a single vortex convecting in a uniform external field and a pair of vortices of opposite strength convecting in their mutual velocity fields. Both cases were strong tests because the translating velocity of each vortex was much less than that of the maximum velocity of the flow around the vortex (at the edge of the core). Thus, the numerical effects of this self-induced velocity had to cancel very accurately to obtain accurate translational velocities.

In both cases, a 128×128 cell grid was used. Also, outer boundary conditions were set based on the computed centroids of the vortices. A second-order, centered convection method was used. Confinement parameters used were $\varepsilon = 0.15$ and $\mu = 0.10$.

1. *Single Vortex*

In the first case (not shown), a single vortex moved in a uniform velocity field, $u_\infty = 0.03$ and $v_\infty = 0.04$ (normalized by the maximum velocity at the edge of the vortex core). The Courant–Friedrichs–Lewy (CFL) number based on this same velocity was 0.4. After 5000 time steps, the vortex core was the same size as it was initially; the contour of one-quarter maximum vorticity (which remained constant) maintained a diameter of ~3 grid cells. During the computation, the vortex should have traveled 60 cells in the x direction and 80 in the y direction (for a total travel of 100 cells). In the computation, the point of maximum vorticity in contour plots was less than one cell from the predicted position. This was expected because it can be easily shown that the centroid will move at the correct velocity if the method conserves momentum (which it did).

2. *Vortex Pair*

In the second case, the two vortices were at 45 deg, with centers initially 10 grid cells apart. (See Fig. 1, where vorticity contours are plotted.) The CFL number was 0.2 and, again, 5000 time steps were used. Based on their separation (with no external flow) their predicted total translation was 70.7 grid cells in both the x and y directions.

The actual translations, again based on the points of maximum vorticity, was within a grid cell of that predicted. Also, as can be seen in Fig. 1a, their separation remained constant. Furthermore, as can be seen in Fig. 1b, the outer (one-quarter maximum vorticity) contour also had a diameter of ~3 grid cells. Note that the unsymmetric appearance of the contours is a figment of the contour plotting software because the center was not at a cell node or cell center and the vorticity varied by $\mathcal{O}(1)$ in 1–2 cells. At time steps where the center was near a cell center or node, the contours were symmetric about the vortex joining line and the line of travel and close to axisymmetric.

B. Computation of Fuselage Flow

The next objective was to quantify the model used for treating body surfaces in Cartesian grids, In particular, the ability to predict surface pressure distributions accurately. First, predicted flow is compared to the exact solution for a (simplified) two-dimensional circular cylinder case. Then, predicted surface pressures at various streamwise stations for a helicopter fuselage are compared to wind-tunnel data.

1. *Two-Dimensional Circular Cylinder*

First, results of a basic study of the flow equations: momentum and mass conservation, without the convective term, are presented

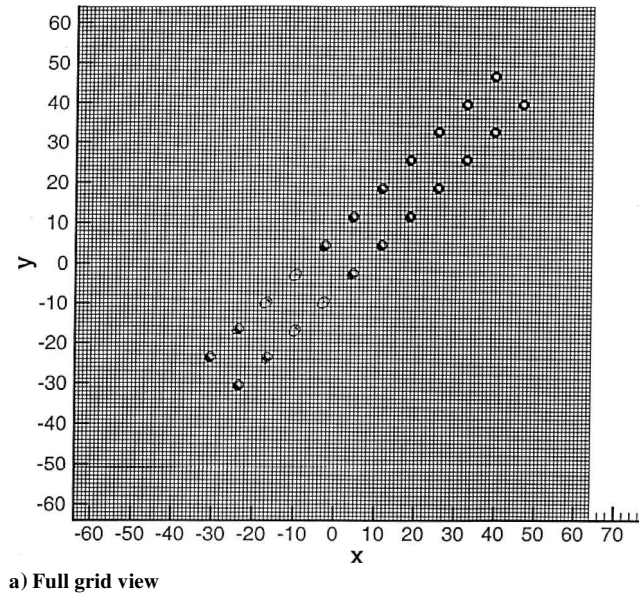

a) Full grid view

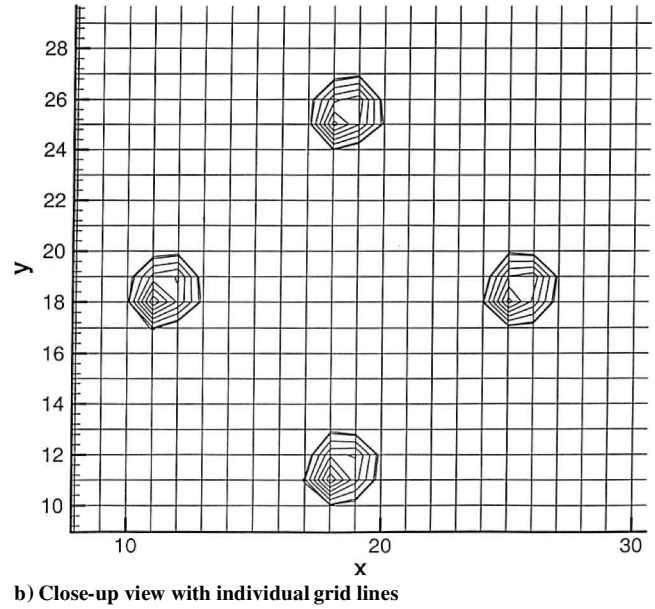

b) Close-up view with individual grid lines

Fig. 1 Vorticity contours of translating vortices.

for flow over a two-dimensional circular cylinder. This is essentially a Cauchy–Riemann solution with attached flow, for which the exact solution is known. This study is important because it validates the basic method of embedding the bound vorticity in a regular Cartesian grid. It tests the accuracy of the method for attached flow in a very precise way.

In these cases, which involved a uniform Cartesian grid, the cylinder was impulsively started from rest. At convergence, the divergence of the velocity field $\boldsymbol{q}$ was zero everywhere, and the vorticity was zero except for a narrow band near the surface. Also, $\boldsymbol{q}$ was zero inside the cylinder.

Streamlines of the computed solution are presented in Fig. 2 for three different grid resolutions across the cylinder diameter: 16, 32, and 64 cells, respectively. The (numerical) displacement thickness effect of the vortical layer is clearly seen. Computed surface velocity (related to pressure by Bernoulli's relation), together with the exact solution, is shown in Fig. 3 as a function of angle about the center of the cylinder. For these results, an extrapolation, discussed hereafter, was used from outside the vortical layer to the surface. It can be seen that the computed results are very accurate, even for the case with 16 grid cells across the cylinder diameter.

Because the vorticity is concentrated about the cylinder surface ($F = 0$), the velocity is rapidly varying there. Because we use

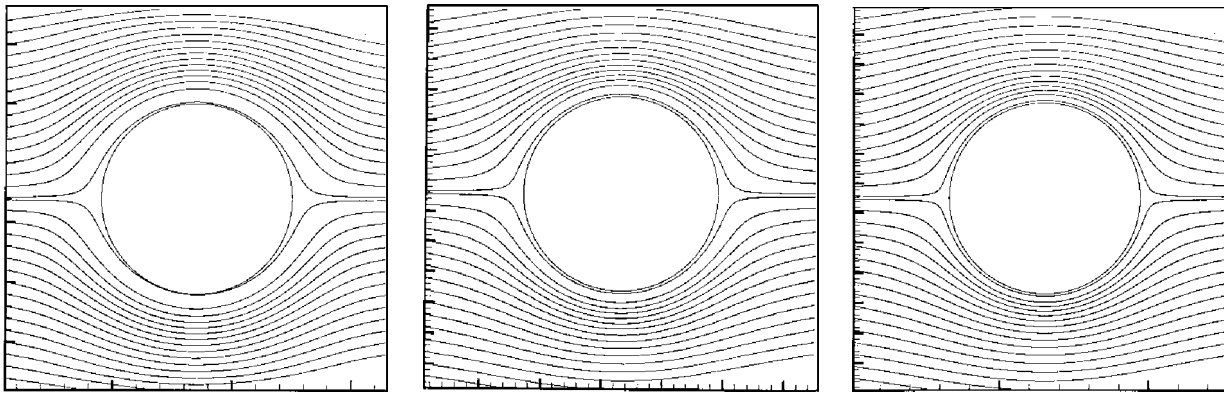

a) 16 cells b) 32 cells c) 64 cells

Fig. 2 Computed streamlines about circular cylinder for various grid resolutions.

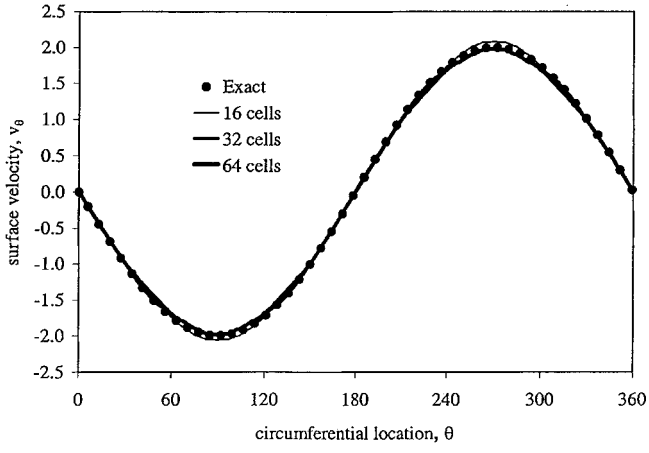

Fig. 3 Comparison of surface velocity predictions with exact solution for two-dimensional circular cylinder.

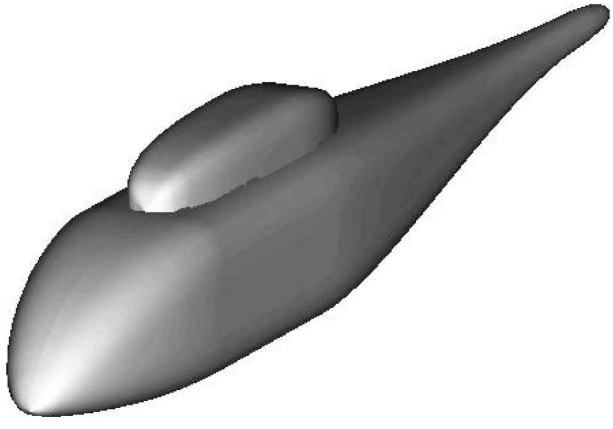

Fig. 4 Surface definition of the ROBIN fuselage.

Bernoulli's relation to compute pressure, we must have a method to extrapolate velocity (or computed pressure) from outside the vortical region where the flow is smoothly varying onto the surface. This extrapolation utilizes vorticity confinement and is described in Refs. 19 and 24. The velocity can then be interpolated onto a set of points that lie on the actual body surface and the pressure computed.

2. Computation of Flow over ROBIN Fuselage

Next, the new extrapolation procedure was evaluated for flow about the ROBIN fuselage (without a rotor), for which extensive wind-tunnel data exist.[25] The fuselage shape is mathematically

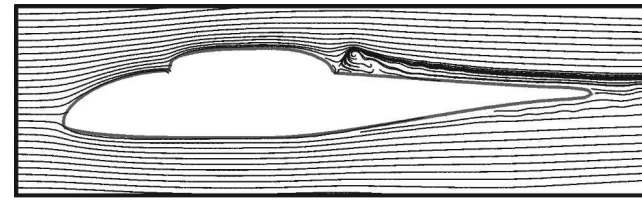

Fig. 5 Computed streamlines along midplane of the ROBIN fuselage (α = 0.0 deg).

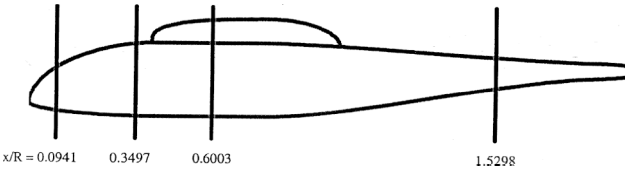

Fig. 6 Cross section of midplane of ROBIN fuselage showing stations used for surface pressure coefficient comparison of predictions with wind-tunnel data.

defined by superellipseequations, which are given in Ref. 25 (Fig. 4). Computations were done for an angle of attack $\alpha = 0$ deg and Reynolds number of 4.5×10^6. Comparisons with wind-tunnel data are presented in this section. The regular Cartesian grid used for these predictions had $(193 \times 49 \times 57)$ cells, and each of the two computations required 2.5 h on an Intel Pentium II, 266-MHz personal computer. A first-order upwind method was used for convection, which had diffusion. No explicit diffusion was added ($\mu = 0$), and ε was set to 0.1.

Computed streamlines in the midplane of the $\alpha = 0$ deg computation are shown in Fig. 5. The streamline paths behind the canopy show separation, as expected. This demonstrates the ability of the method to treat separation. (This is obviously qualitative; a detailed comparison is, of course, required to demonstrate quantitative prediction for this separated flow.) A cross section of the fuselage along the midplane around the body is shown in Fig. 6. Figure 6 shows the locations where the predicted surface pressure coefficients are presented. For $\alpha = 0$ deg, the comparison of predicted surface pressures with data is good, as can be seen in Fig. 7.

In general, the surface pressure predictions also agree well with a panel method and Navier–Stokes predictions.[26] (These are not shown in Fig. 7.) By contrast, the panel method can not treat general separating flows, and the Navier–Stokes method, for general bodies, requires a lengthy procedure to generate body-conforming grids that require very long computational times. We conclude that vorticity confinement can serve as the basis of a simple, efficient method for accurately modeling the flow about body surfaces. As in conventional Reynolds-averaged turbulence modeling, other terms with empirically determined coefficients could be used to further

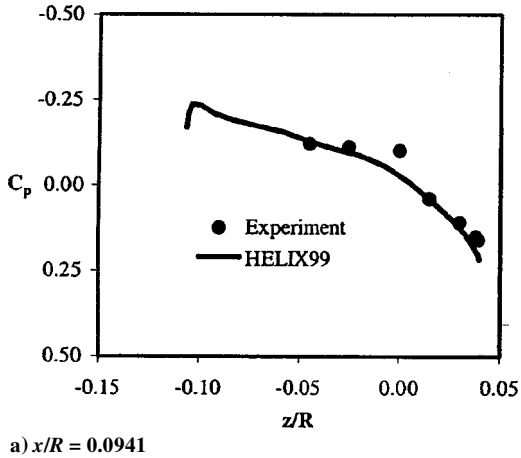

a) $x/R = 0.0941$

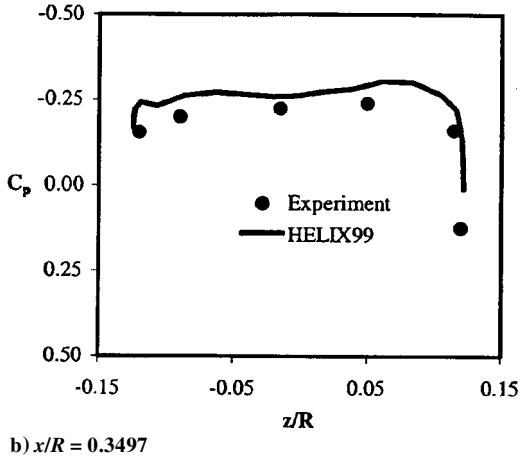

b) $x/R = 0.3497$

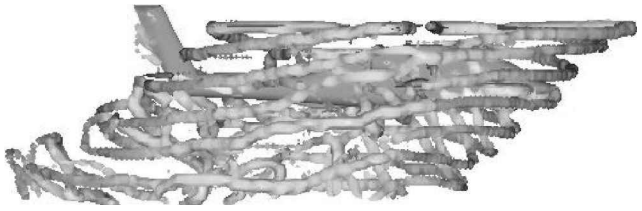

Fig. 11 Side view of the computed vorticity isosurfaces for the Apache helicopter including main rotor blades (HELIX99, low advance ratio).

V. Conclusions

The method presented in this paper, based on vorticity confinement, has been shown to solve two important incompressible flow problems: the computation of convecting concentrated vortices over long times with no numerical spreading and the computation of flow over complex bodies without body-conforming grids or long setup times. Most of the computations were completely Eulerian and only required a coarse, regular computational grid.

The new method involves generating solitary wavelike configurations on the computational lattice to represent vortical regions. These are direct solutions of nonlinear difference equations, rather than solutions of conventional discrete finite difference approximations to PDE models for these regions. In the irrotational regions, the method automatically reverts to a standard finite difference one. As such, the new method provides a new, efficient framework for efficiently computing a large class of flows.

Of course, as with conventional methods, much work remains to be done for validation and calibration of models for Reynolds-averaged representations of turbulent regions. We are currently developing such models, which are quite different from conventional PDE models.

Acknowledgments

Development of the method and the work presented here were partially supported by the U.S. Army Research Office, the U.S. Army Aeroflightdynamics Directorate, NASA, and U.S. Army Small Business Innovation Research Grants, as well as the University of Tennessee Space Institute. We express our gratitude to Frank Caradonna of the Army Aeroflightdynamics Directorate at Moffett Field for extensive advice on rotorcraft aerodynamic issues. We also thank anonymous reviewers for helpful comments.

References

[1]Ahmad, J. U., and Strawn, R. C., "Hovering Rotor and Calculations with an Overset-Grid Navier–Stokes Solver," *Proceedings of the American Helicopter Society 55th Annual Forum*, American Helicopter Society, Alexandria, VA, 1999, pp. 1949–1959.

[2]Steinhoff, J., Senge, H., and Wenren, Y., "Computational Vortex Capturing," Univ. of Tennessee Space Inst., Preprint, Tullahoma, TN, 1990.

[3]Steinhoff, J., and Underhill, D., "Modification of the Euler Equations for Vorticity Confinement Application to the Computation of Interacting Vortex Rings," *Physics of Fluids*, Vol. 6, 1994, pp. 2738–2743.

[4]Rosenhead, L., *Proceedings of the Royal Society of London, Series A: Mathematical and Physical Sciences*, 134, 1931, pp. 170–192.

[5]Westwater, F. L., *Reports and Memoranda*, No. 1692, 1936.

[6]Krasny, R., "Vortex Sheet Computations: Roll-Up, Wakes, Separation," *Lectures in Applied Mathematics*, Vol. 28, 1991. p. 383.

[7]Leonard, A., "Vortex Methods for Flow Simulation," *Journal of Computational Physics*, Vol. 37, No. 3, 1980, pp. 289–335.

[8]Helmholtz, H. von., "On the Discontinuous Motion of Fluids," *Philosophical Magazine*, Ser. 4, No. 36, 1868, p. 337.

[9]Kirchhoff, G., "On the Theory of Free Fluid Jets," *Jour. fur die Reine und Angew. Math.*, Vol. 70, 1869, p. 289.

[10]Dindar, M., Lemnios, A. Z., Shephard, M. S., Flaherty, J. E., and Jansen, K., "An Adaptive Solution Procedure for Rotorcraft Aerodynamics," AIAA Paper 98- 2417, 1998.

[11]Van Dommeln, L. L., and Shen, S. F., "The Spontaneous Generation of the Singularity in a Separating Laminar Boundary Layer," *Journal of Computational Physics*, Vol. 38, No. 2, 1980, pp. 125–140.

[12]Steinhoff, J., Puskas, E., Babu, S., Wenren, Y., and Underhill, D., "Computation of Thin Features over Long Distances Using Solitary Waves," *Proceedings of AIAA 13th Computational Fluid Dynamics Conference*, AIAA, Reston, VA, 1997, pp. 743–759.

[13]Steinhoff, J., Wang, C., Underhill, D., Mersch, T., and Wenren, Y., "Computational Vorticity Confinement: A Non-Diffusive Eulerian Method for Vortex-Dominated Flows," Univ. of Tennessee Space Inst., Preprint, Tullahoma, TN, 1992.

[14]Steinhoff, J., "Vorticity Confinement: A New Technique for Computing Vortex Dominated Flows," *Frontiers of Computational Fluid Dynamics*, edited by D. Caughey and M. Hafez, Wiley, New York, 1994, pp. 235–264.

[15]Pevchin, S. V., Steinhoff, J., and Grossman, B., "Capture of Contact Discontinuities and Shock Waves Using a Discontinuity Confinement Procedure," AIAA Paper 97-0874, 1997.

[16]Steinhoff, J., Mersch, T., and Wenren, Y., "Computational Vorticity Confinement: Two Dimensional Incompressible Flow," *Proceedings of the Sixteenth Southeastern Conference on Theoretical and Applied Mechanics*, Beaver Press, Manchester, TN, 1992, pp. III.II.73–III.II.82.

[17]Fan, M., Wenren, Y., Dietz, W., Xiao, M., and Steinhoff, J., "Computing Blunt Body Flows on Coarse Grids Using Vorticity Confinement," *Journal of Fluids Engineering*, Vol. 124, Dec. 2002, pp. 876–885.

[18]Underhill, D., "Investigation of the Vorticity Confinement Method for Flows with Separation," Ph.D. Dissertation, Univ. of Tennessee Space Inst., Tullahoma, TN, May 1997.

[19]Steinhoff, J., Wenren, Y., and Wang, L., "Efficient Computation of Separating High Reynolds Number Incompressible Flows Using Vorticity Confinement," AIAA Paper 99-3316, 1999.

[20]Steinhoff, J., et al., "Vorticity Confinement: A Survey of Recent Results," Proceedings of 1st Annual ARO Workshop on Vorticity Confinement and Related Methods, Univ. of Tennessee Space Inst., Preprint, Tullahoma, TN, May 1996.

[21]Steinhoff, J., et al., Proceedings of 2nd Annual ARO Workshop on Vorticity Confinement and Related Methods, Univ. of Tennessee Space Inst., Preprint, Tullahoma, TN, May 1997.

[22]Steinhoff, J., et al., Proceedings of 3rd Annual ARO Workshop on Vorticity Confinement and Related Methods, Univ. of Tennessee Space Inst., Preprint, Tullahoma, TN, Nov. 1998.

[23]Kim, J., and Moin, P., "Application of a Fractional-Step Method to Incompressible Navier–Stokes Equations," *Journal of Computational Physics*, Vol. 59, No. 2, 1985, pp. 308–323.

[24]Steinhoff, J., Wenren, Y., Wang, L., Fan, M., Xiao, M., and Braun, C., "Application of Vorticity Confinement to the Prediction of the Wake of Helicopter Rotors and Complex Bodies," *Computational Fluid Dynamics Journal*, Vol. 9, April 2001, pp. 699–707.

[25]Freeman, C. E., and Mineck, R. E., "Fuselage Surface Pressure Measurements of a Helicopter Wind Tunnel Model with a 3.15-Meter Diameter Single Rotor," NASA TM-80051, March 1979.

[26]Chaffin, M. S., and Berry, J. D., "Navier–Stokes and Potential Theory Solutions for a Helicopter Fuselage and Comparison with Experiment," NASA TM-4566, 1994.

K. Kailasanath
Associate Editor